

ANALYTICAL MODELS FOR SHOCKS IN TRANSONIC FLOW

Helmut Sobieczky

DLR German Aerospace Center, Bunsenstr. 10, Göttingen, 37073 Germany

Summary Objective is trying to maintain the value of analytic modelling for deeper insight, education and development of new design concepts. Analytical flow models are used to confirm wellknown and find new solutions: Logarithmic structure of surface pressure distribution occurs with occurrence of different shock waves interacting with contour geometry.

MAPPING THE FLOW PROBLEMS TO THE HODOGRAPH

A recent IUTAM symposium [1] on transonic flow has shown that analytic treatment of complex flows still draws interest as an efficient tool to shed light into complex flow details where numerical results give no clear answers. Complexity of flow problems may stem from special boundary conditions as well as from dynamics within the flow field. In transonic flow, the latter source of complexity, for instance, occurs due to shock waves within the flow field. This holds already for steady, inviscid 2D flow. Aerodynamic applications, of course, require the simulation of steady and unsteady viscous and 3D flows, but with recent developments in flow control technology, as seen in [1], prescribing target pressure distributions to control viscous interaction becomes important. We are therefore interested to preserve some of the findings from inviscid, 2D flows models, guiding us to suitably parameterize design parameters.

Here we use the idealized 2D near sonic flow equations (1) for velocity components U , V describing perturbed sonic velocity parallel flow ($U = 0$, $V = 0$). These equations model potential flow for vorticity $\omega = 0$ and also represent a small perturbation approximation of the Euler equations. For $\omega = 0$ the hodograph transformation to velocity variables v, θ (Prandtl-Meyer angle, $v \sim \pm|U|^{3/2}$, and flow angle θ) results in the Beltrami mapping equations (2). We note that this system is linear and weakly singular at $v = 0$, it is the basis for near sonic flow phenomena modelling. Investigation of flow phenomena, which do not include the sonic condition $v = 0$, but focus around perturbing a special value of v , lead to simple Cauchy-Riemann (C-R) or wave equations (3) in the hodograph plane. This is equivalent to suitably linearizing (1) around a given value of $U \neq 0$ and this way also obtaining C-R or wave equations in the (X, Y) physical plane.

$$\boxed{U \cdot U_X - V_Y = 0 \qquad U_Y - V_X = \omega} \quad (1)$$

$$\boxed{X_v = v^{1/3} \cdot Y_\theta \qquad X_\theta = \pm v^{1/3} \cdot Y_v} \quad (2)$$

$$\boxed{X_v = \pm Y_\theta \qquad X_\theta = Y_v} \quad (3)$$

A wellknown example: Normal shock on the curved wall (See also the illustrations in the Appendix!)

A series of publications has dealt with the problem of a normal shock on a curved wall. A study of the relevant milestones which confirmed the analytical structure of a logarithmic solution for the pressure distribution along the wall, $c_p \sim a+bX \log(X)+\dots$, should start with the work of v.Koppenfels [2] about incompressible flow past walls with curvature jumps. Emmons [3] numerically solved the compressible flow Euler equations and mentions qualitative relations of his results to flows as investigated by v.Koppenfels. Gadd [4] clearly points out this earlier work to arrive at a logarithmic model, Oswatitsch and Zierp [5] confirm the logarithmic solution by studying the above equation (1), linearized around the value of U behind a normal shock and without vorticity. Final doubts about validity of such local potential solution, based on the occurrence of shock-curvature-induced vorticity, are removed by Fung [6] concluding that the vorticity terms are of a higher order than those governing the logarithmic character of the solution.

Finally, our own work in transonic airfoil design fits to this model, if a shock is being designed using the Fictitious Gas technique: Sobieczky and Niederdrenk [7] use subsonic initial boundary conditions with a curvature jump to solve an elliptic ("fictitious") boundary value problem, before in a second step a supersonic flow pattern terminated by a shock wave and the smoothly curved contour wetted by supersonic flow is constructed by the method of characteristics and the shock relations. Such academic examples led us to develop novel wing design strategies, to be applied subsequently to 3D, viscous and even unsteady aerodynamics. Examples are shown in [1].

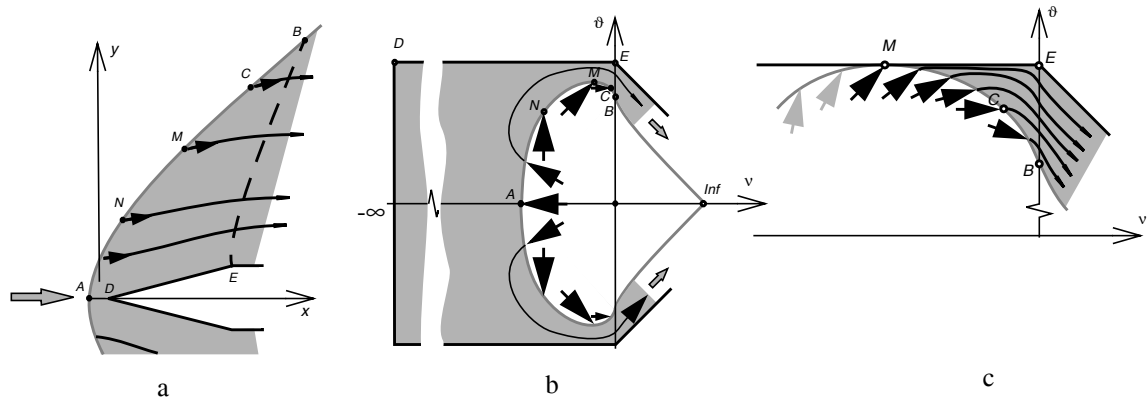
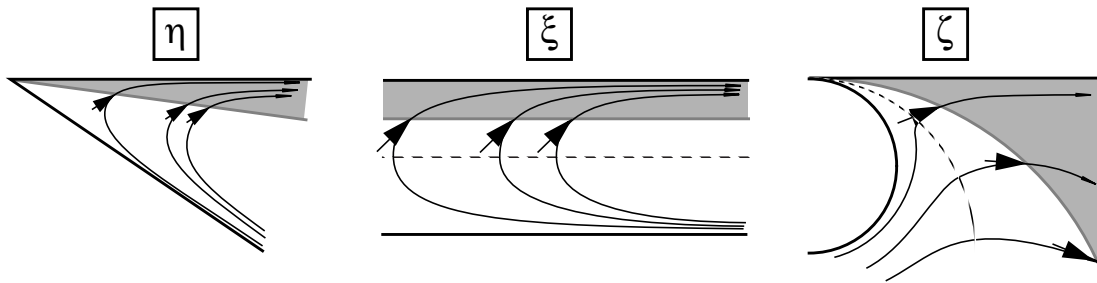


Fig. 1: Shock attachment to a wedge in low supersonic Mach number flow (a), analog to growing shock polar with flow emanating under given directions in hodograph plane (b) until touching fixed contour DE, (c).



$$Z = X - iY = \eta^n \quad \eta = e^\xi \quad \zeta = (v - v_M) + i(\vartheta - \vartheta_M) = 1/\xi$$

Fig. 2: Conformal mappings to find solution $\zeta = \text{Fct}(Z)$, resulting in wedge surface pressure $c_p(v) = \text{fct}(X)_{Y=0}$

Another logarithmic flow singularity: shock attaching to a wedge airfoil leading edge

Here another problem is presented involving the shock relations near a singular location on the boundary: Shock attachment to a wedge leading edge (Fig. 1a) requires a transition from a detached normal shock to an oblique shock. This problem is treated easier in the hodograph plane (Fig. 1b) using the Beltrami mapping system (2), the shock polar and investigating the vicinity of the shock polar maximum deflection point M (Fig 1c). This allows for linearization around the subsonic v_M using C-R system (3). With systems (2) and (3) representing analog flow in the hodograph plane (v, ϑ), we have to describe a potential flow model in the sharp angle left of M, with a straight solid boundary above and a curved transpiring boundary with flow emanating under 45° from it. For solution of this boundary value problem a series of simple conformal mappings is used and illustrated in Fig. 2. From these the pressure coefficient along the wedge contour near the tip results to $c_p \sim a + b/\log(X) + \dots$, obviously a hitherto not yet described detail of shock attachment to a wedge.

CONCLUSION

Analytical flow models are still seen as precise tools to: (1) understand complicated flow patterns generated by special boundary conditions, (2) subsequently explain and educate about flow phenomena and (3), finally use their suitably parameterized mathematics for aerospace design and optimization.

References

- 1 Sobieczky, H. (Ed.): Proc. IUTAM Symposium Transsonicum IV. Kluwer Acad. Publ., Dordrecht 2003
- 2 v.Koppenfels, W.: Luftfahrtforschung Bd. 17, Lfg. 7, (1940), translated in NACA TM 996, 1941
- 3 Emmons, H. W.: Flow of a Compressible Fluid past a Symmetrical Airfoil. NACA TN 1746, 1948
- 4 Gadd, G. E.: The Possibility of Normal Shock Waves on a Body with Convex Surfaces in Inviscid Transonic Flow. ZAMP 11, 1960
- 5 Oswatitsch, K., Zierep, J.: Das Problem des Senkrechten Stosses an einer Gekrümmtten Wand. ZAMM 40, 1960
- 6 Fung, K.-Y.: Vorticity at the Shock Foot in Inviscid Flow. AIAA Journal 21, No. 6, 1983
- 7 Sobieczky, H., Niederdrenk, P.: Entwurf einer Transsonischen Strömung mit Verdichtungsstoss ZAMM 65, 1985.

APPENDIX: Illustrations from a Poster Seminar

Topic:

Elliptic continuation for design of transonic flows with and without Recompression Shock

Incompressible flow

$$\begin{aligned} U_X + V_Y &= 0 \\ U_Y - V_X &= 0 \end{aligned}$$

Velocity distribution singularity
near curvature discontinuity F

$$\bar{w} - \bar{w}_F = a \cdot z + b \cdot z \cdot \ln(z) + \dots$$

$$\bar{w}_F = u_F - i \cdot v_F$$

Near sonic flow

$$\begin{aligned} U_X - V_Y &= 0 \\ U_Y - V_X &= \omega \end{aligned}$$

Shock at x_F :

$$c_p(x > x_F) - c_{pF} \sim (x - x_F) \cdot \ln(x - x_F) + \dots$$

Vorticity ω generated at shock,
swept downstream:

does it change singularity?

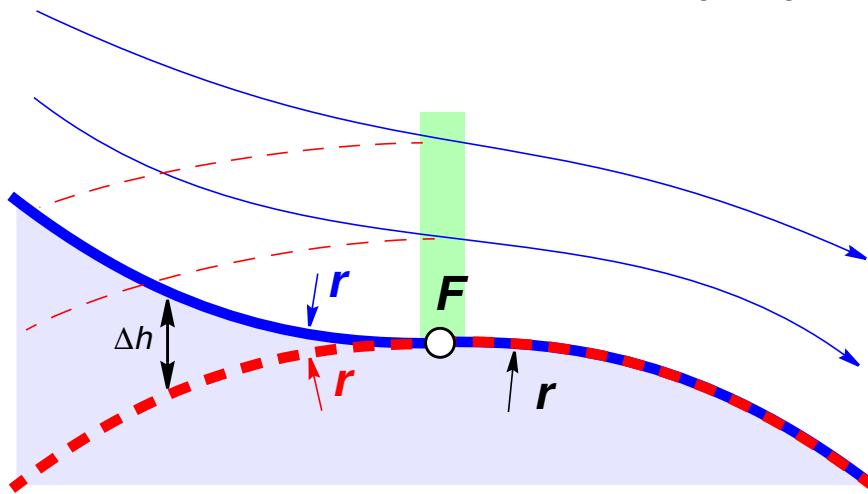


Figure A1: Flow models with logarithmic singularity

Here we show flow elements requiring analytical modelling to understand the velocity or pressure distribution near special points along the curved boundary:

W. v.Koppenfels (1941) investigated potential flow past a wall with curvature discontinuity and found that a logarithmic function allows for observing this special boundary condition in inviscid flow. (See the blue contour and streamline sketches, below the basic potential equation for incompressible flow).

As we will see from the following outline, this flow downstream of a singular point F models also a compressible subsonic potential flow past a continuously curved boundary, as it occurs on a convex airfoil. The flow upstream of point F therefore consists of another flow element, which is a supersonic potential flow, see the red dashed contour and streamline! The upstream supersonic and downstream subsonic portion of the flow are connected by a shock discontinuity, as illustrated here by the green shaded band, so far leaving open the precise shape of the shock. The simplest analytic description is performed by solving the near sonic equation.

In the next illustration we show that the basic logarithmic flow model for the flow with shock was first suggested, later derived and confirmed by various authors during the second half of the 20th century.

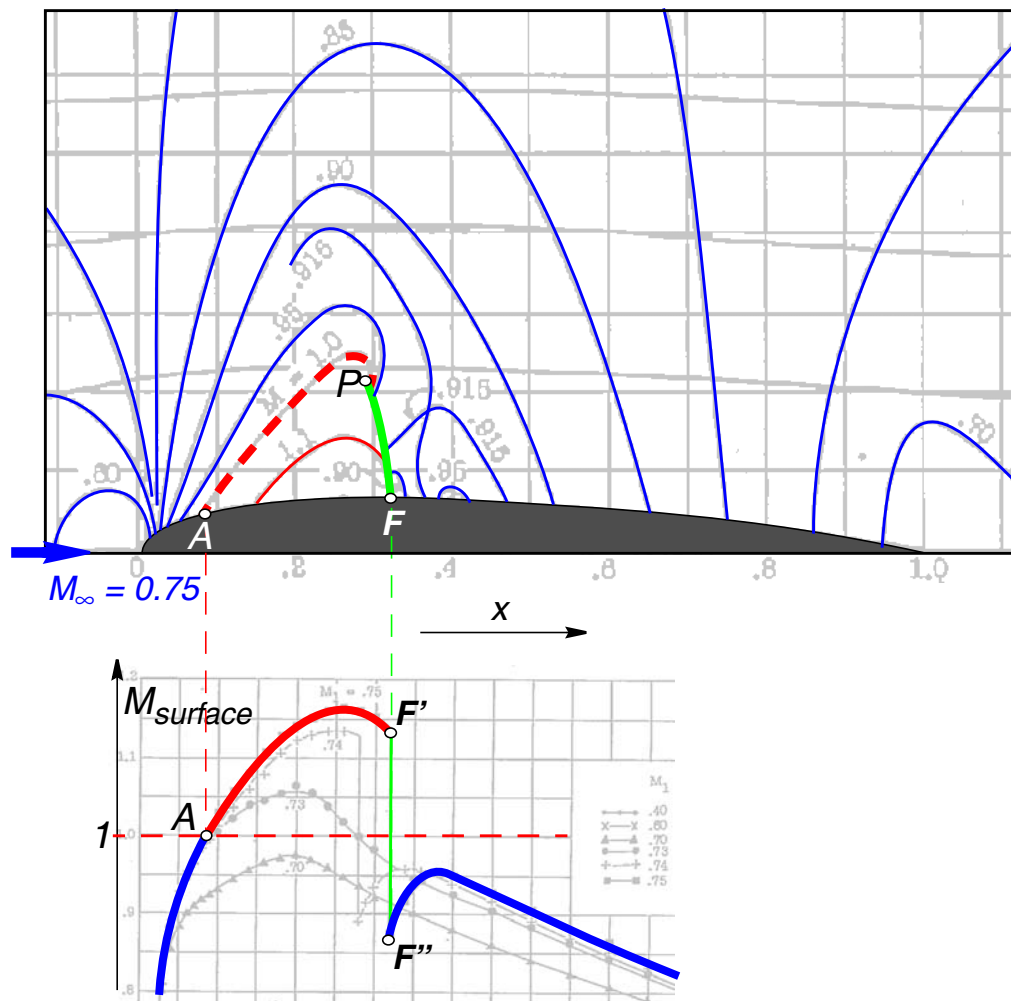


Figure A2: The first numerical simulation of transonic airfoil flow

Figure A2 shows the first evaluation of transonic airfoil flow (using early numerical calculators), published by **H. Emmons** in 1948, (*“Emmons plus 300 girls”*). The Euler equations, modelling inviscid, compressible flow include an accurate simulation of the shock relations; the high resolution of Emmons’ calculation allowed for an early correct simulation of the local supersonic domain, with smooth acceleration in surface point A, the shock formation within the supersonic domain close to the sonic line (point P), as well as the curved, normal ending of the shock on the surface (point F). For decades after publication of this result, theoretical models for transonic flow with mathematically possible interaction of sonic line, shock and bounding surface were presented, most of them yielding unrealistic solutions ignoring Emmons’ detailed results. Moreover, it was Emmons himself who already pointed out the relation of the numerical result obtained for the shock to the v. Koppenfels flow model illustrated before. This was clearly acknowledged and mathematically proven, again for the Euler equations, by **G. Gadd** in 1960. A local solution of the equation for near sonic flow, as depicted in the above illustration (Figure A1), by **K.Oswatitsch** and **J. Zierep** in 1960 show the same logarithmic model for potential flow, i. e. without the vorticity term ω . Later, **K-Y. Fung** (1983) shows that the potential flow model indeed is sufficient to predict the logarithmic solution by proving that the shock induced vorticity in the downstream portion of the flow is of higher order effect to influencing the mathematical structure of the solution.

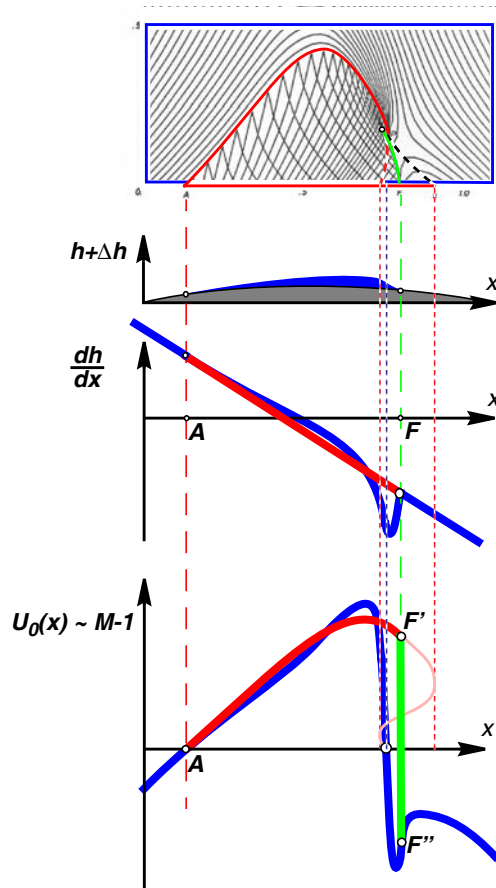


Figure A3: Using Elliptic Continuation for the construction of a transonic flow with shock

In the late 1970's, building on the transonic flow modeling knowledge base including the above-mentioned understanding of shock waves on a curved surface, the present author developed a method to construct examples of transonic flows, to be applied in practical aerodynamic design techniques. These efforts resulted in a concept to design aircraft airfoils and wings which do not have recompression shocks and therefore show higher aerodynamic efficiency. For the purpose of demonstrating the consistency of this concept then using already CFD methods, with the analytical flow models as outlined above also airfoil flows with recompression shocks were designed (Sobieczyk and Niederdrenk, 1984). Formulation of the related boundary value problems makes use of a temporary analytic continuation of the subsonic flow field into the supersonic domain by locally changing the gasdynamic equations of state. In its simplest form this results in replacing the nonlinear term $U \cdot U_x$ in the near sonic equation (see Figure A1) by $-|U| \cdot U_x$ which keeps the equation correct if $U < 0$ and changes the flow model to a "fictitious" one where there should be supersonic flow. Analogous to the flow parameters also the boundary conditions within the analytic continuation may be altered: Here we remember that the subsonic v.Koppenfels solution with wall curvature discontinuity and the transonic flow element with shock along a smoothly curved wall differ by $\Delta h \sim (x-x_F)^2 + \dots$ in the upstream direction.

Figure A3 illustrates the 3 steps to "design" the near sonic flow past a wall with constant curvature. A finite difference method solving the near sonic equation with manipulated nonlinear term to first get the subsonic flow was used. Subsequently the method of characteristics provides the still missing correct supersonic part of the flow, including an overlapping into the subsonic domain; and finally the shock relations could be used to fit together the two flow patterns where they overlap. Of course, choice of the range and quantity $\Delta h(x)$ controls the whole solution, but its quality near the shock is given by the above quadratic term.

Shock design:

Step 1: Obtain an all-elliptic solution past a deformed boundary $h+\Delta h$ including a sonic line $U=0$.

Method: numerically solve equation $|U| \cdot U_x + V_y = 0, U_y - V_x = 0$.

B.C. needs curvature discontinuity for later accommodating shock singularity

Step 2: Use initial data along sonic line to solve correct supersonic flow within local domain where $U > 0$.

Method: Numerical cross marching (Method of Characteristics) toward B. C. Result is a supersonic flow pattern with new distribution ($U > 0, V$), partly overlapping subsonic solution ($U > 0$).

Step 3: Integrate shock shape by cutting subsonic and supersonic pattern in overlap region, starting at characteristics coalescing point.

Method: Apply shock relations for ΔU and shock inclination.

Tuning of B.C. deformation Δh is needed to yield given $h(x)$, arrive with shock integration at curvature jump and partly replace surface velocity U_0 .

Fictitious Gas (Elliptic Continuation)

Boundary condition differences

$$\text{Exact: } \Delta h = \int_{\zeta_S}^{\zeta_C} (\rho_f - \rho(q_f)) q_f d\zeta / (\rho_f q_f)_C$$

$$\text{Approx.: } \Delta h / \Delta h_{\max} \sim (\sin(\pi F(X)))^{3-k} \sin(\pi F(X))$$

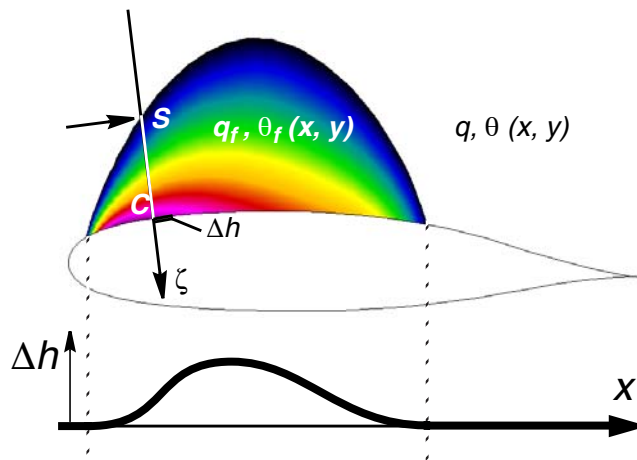


Figure A4: Surface modifications resulting from Fictitious Gas Design

Computational simulation of desirable flow properties making use of elliptic continuation, i. e. the preliminary computation of a partly fictitious all-elliptic flow has profited from analytical models like the ones shown above. Other than modeling flows with shocks, however, practically useful airfoils were sought to be shock-free in certain operating conditions, so that the models with shock rather serve only as educational tools helping to clarify the old transonic controversy: How isolated is shock-free flow within flows where generally shock waves occur? With analytical models and mapping techniques to hodograph variables (see equations (2), (3) in the present paper) this question seems to have been answered completely.

Our own efforts to design shock-free configurations use the differences between physical supersonic solutions and analytical subsonic continuations to define gasdynamic parameters which would give physical meaning to an otherwise only fictitious support procedure: Distributed energy removal and re-injection along the streamlines serve as a good explanation to control the flow to stay subsonic despite reaching velocities beyond the critical speed of sound. Different successful applications of this concept by various authors are outlined in the book **Sobieczky (Ed.), 2003**. The illustration above is intended to show how surface differences for fictitious and real airfoil flows with common subsonic and sonic flow quality are related to density differences: Integration of the flux results in different surface boundaries, which helps to calibrate parameterized bumps to be added or subtracted from given contours. For shock-free flow these bumps have starting and ending ramps of 3rd order parabolas, thus being of smooth curvature. For shock design we have seen that the bump ramp is of 2nd order, modelling the discontinuous curvature for accommodating the logarithmic flow singularity at the shock foot point.

Numerical airfoil optimization
Parametric surface definition with
reduced number of parameters
based on model flow experience

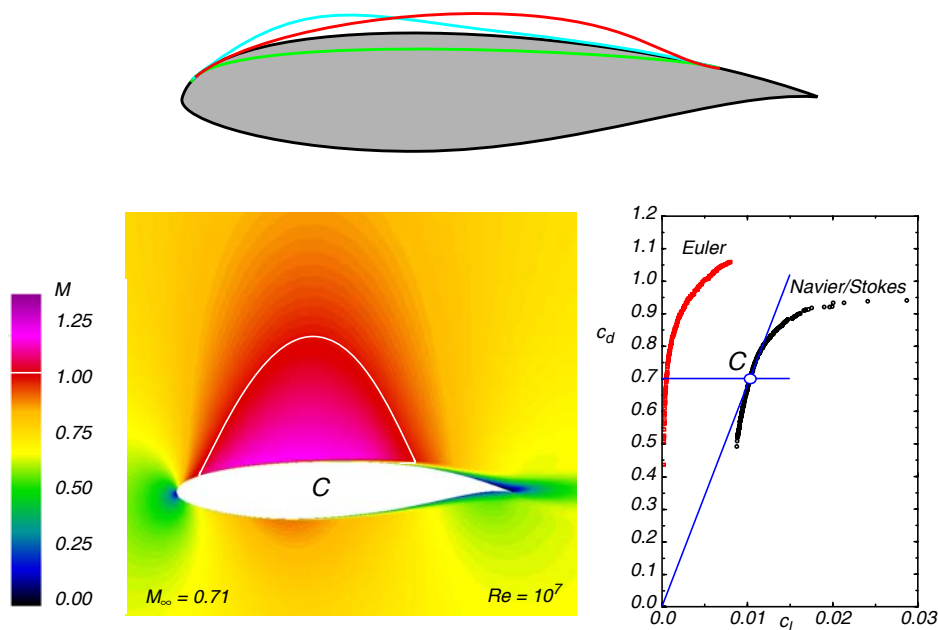


Figure A5: Airfoil input data variation for design optimization

Presently we already have computational analysis codes for compressible, viscous flow and optimization strategies have been developed so that every rational design philosophy may accelerate design optimization remarkably.

In this situation the availability of rapid parametric geometry variations to aerodynamic baseline configurations becomes crucial for efficient design. Our activities have therefore focused on geometrical modelling rather than flow modelling: The fluid dynamics and aerodynamics knowledge base point toward becoming very flexible in shape definition in 3D space and, moreover, in 4D shape morphing for adaptive components, unsteady configurations or optimization variations.

The above Figure A5 shows the result of a shock-free transonic airfoil flow obtained by **M. Klein (2001)** using a genetic algorithm optimization and an Euler /Navier-Stokes CFD code. The illustration also depicts Pareto fronts of this optimization study showing results for a whole family of airfoil without or with minimized shock, represented by lift and drag coefficients, c_l and c_d . The selected example “C” shown with Mach number isofringes comes close to the best of all found airfoils with a maximum ratio c_l and c_d .

All airfoil geometries are generated with a limited number of suitable parameters, their definition guided by our previous experience with analytical boundary conditions.

For related work see: <http://www.as.go.dlr.de/~helmut>